Journal of Photochemistry and Photobiology A: Chemistry 205 (2009) 44–50

Contents lists available at ScienceDirect

Journal of Photochemistry and Photobiology A: Chemistry

journal homepage: www.elsevier.com/locate/jphotochem

Photochemistry and absorption cross-sections temperature dependence of trifluoromethoxycarbonyl peroxy nitrate ($CF_3OC(O)OONO_2$)

F.E. Malanca*, M.D. Manetti, M.S. Chiappero, P. Gallay, G.A. Argüello

INFIQC, Departamento de Fisicoquímica, Facultad de Ciencias Químicas, Universidad Nacional de Córdoba, Ciudad Universitaria, 5000 Córdoba, Argentina

ARTICLE INFO

Article history:
Received 18 November 2008
Received in revised form 3 April 2009
Accepted 9 April 2009
Available online 18 April 2009

Keywords:
Quantum yield
Peroxy nitrates
Trifluoromethoxycarbonyl peroxy nitrate
Absorption cross-sections
Temperature dependence

ABSTRACT

The photochemical rupture of $CF_3OC(O)OONO_2$ at 254 nm leads to the formation of $NO_2 + CF_3OC(O)OO$, and $NO_3 + CF_3OC(O)O$ radicals. The study carried out at 297, 273 and 253 K leads to a quantum yield $\phi_{NO_3} = 0.18 \pm 0.03$, and $\phi_{NO_2} + \phi_{NO_3} = 1.01 \pm 0.09$. To minimize the errors in both the determination of quantum yields and the analysis of atmospheric photochemical lifetimes, the study of the absorption cross-sections dependence with temperature between 297 and 245 K was undertaken. There is a clear increase of the cross-sections with temperature. The atmospheric photochemical lifetime of $CF_3OC(O)OONO_2$ and its comparison with thermal decomposition are presented.

© 2009 Elsevier B.V. All rights reserved.

1. Introduction

Peroxynitrates ($ROONO_2$) are important species in the atmosphere because they have relatively long atmospheric thermal lifetimes and consequently can be transported from the sources to remote places or even the stratosphere, acting as reservoirs of NO_2 and ROO radicals [1–3].

Peroxy acetyl nitrate (PAN, $CH_3C(O)OONO_2$), peroxy propionyl nitrate (PPN, $C_2H_5C(O)OONO_2$) and peroxy benzoyl nitrate (PBzN, $C_6H_5C(O)OONO_2$) can be formed in the troposphere as a consequence of hydrocarbon oxidation, and have been detected and measured in the atmosphere [4,5].

Industrial fluorinated molecules as chlorofluorocarbon, hydrofluorochlorocarbon, hydrofluorocarbon and hydrofluoroethers could lead in the atmosphere to the formation of thermally stable peroxy nitrates, as for instance, fluoroformyl peroxy nitrate ($FC(O)OONO_2$), trifluoroacetyl peroxy nitrate ($CF_3C(O)OONO_2$) and trifluoromethoxycarbonyl peroxy nitrate ($CF_3OC(O)OONO_2$) [6].

Precisely, as a consequence of the relatively long thermal lifetimes of peroxynitrates in the atmosphere, especially at higher altitudes where the temperatures are relatively low, the study of the photochemistry of these molecules is relevant, since if they absorb light and react, the actual lifetime is determined by the shorter of the two processes. For these molecules, there are two channels to the photochemical rupture:

$$ROONO_2 + h\nu(\lambda = 254\,nm) \rightarrow ROO + NO_2 \quad (1a)$$

$$ROONO_2 + h\nu(\lambda = 254\,nm) \rightarrow RO + NO_3 \quad (1b)$$

In particular, quantum yields of path 1a (ϕ_{NO_2}) and 1b (ϕ_{NO_3}) for PAN and PPN have been measured by Mazely et al. [7,8], Harwood et al. [9] and Flowers et al. [10] at room temperature and at different wavelengths.

The value of ϕ_{NO_2} reported for PAN at $\lambda = 248$ nm by Mazely et al. [7] is 0.83 ± 0.09. In separate experiments, the same authors reported $\phi_{NO_3} = 0.3 \pm 0.1$ [8]. Other authors reported for the formation of NO_3 radicals, values of 0.19 ± 0.04 [9]; 0.31 ± 0.08 [10]; 0.41 ± 0.10 at 248, 289 and 308 nm, respectively [9]; while for PPN the values reported are 0.22 ± 0.04 and 0.39 ± 0.04 at 248 and 308 nm, respectively [9].

Trifluoromethoxycarbonyl peroxy nitrate has been characterized by von Ahsen et al. [6]. Besides, Christensen et al. [11] determined its thermal stability inside a smog chamber at 295.8 K in a mixture containing NO_2 and NO. More recently Manetti et al. [12] studied its thermal decomposition between 303 and 273 K starting from pure samples.

In this work, we determine the total quantum yield (i.e. $\phi_T = \phi_{NO_2} + \phi_{NO_3}$) as well as the quantum yield of NO_3 (ϕ_{NO_3}) formation in the photolysis of $CF_3OC(O)OONO_2$ at 254 nm. Additionally, UV absorption cross-sections over the wavelength range 200–330 nm between 297 and 245 K have been measured. Estimated photochemical lifetimes as a function of altitude are calculated.

* Corresponding author. Tel.: +54 351 433 4169; fax: +54 351 433 4188.
E-mail address: fmalanca@fcq.unc.edu.ar (F.E. Malanca).

1010-6030/$ – see front matter © 2009 Elsevier B.V. All rights reserved.
doi:10.1016/j.jphotochem.2009.04.003

2. Experimental

2.1. Chemicals

Commercially available samples of perfluoroacetic anhydride $(CF_3C(O))_2O$ (PCR), CO (PRAXAIR), NO (AGA), Helium (AGA) and O_2 (AGA), cyclohexane (Sigma) were used. Perfluoroacetic anhydride was purified by repeated vacuum distillation between 213 and 183 K.

Oxygen was condensed from a flowing stream at atmospheric pressure passing through a trap immersed in liquid air. It was then pumped under vacuum several times and transferred to a glass bulb whilst the trap was still immersed in liquid air. A mixture of NO_2/O_2, used to synthesize the peroxy nitrate, was prepared adding O_2 to NO (ratio 1:10).

$CF_3OC(O)OONO_2$ was synthesized from a mixture of $CF_3OC(O)O_3C(O)OCF_3/NO_2/O_2$. Briefly, the reaction begins when the trioxide decomposes leading to $CF_3OC(O)OO$ radicals that in the presence of NO_2 form the nitrate as described in von Ahsen et al. [6]. Residual NO_2 in the sample was eliminated by adding ozone and further distilling the sample to obtain pure trifluoromethoxycarbonyl peroxy nitrate. Its stability was checked by UV and infrared spectrometry (no disappearance was registered at the higher temperature used (298 K) in the time of our experiments, i.e. 1–2 h).

2.2. Methods

To measure the temperature dependence of the UV absorption cross-sections, the experimental set-up described in Malanca et al. [13] was used. A standard quartz gas cell (length 10 cm) inside an evacuated metal box that allowed the attainment of low temperatures without condensation problems was placed in the optical path of a diode array detector UV–vis spectrometer. With this set-up and the use of a cryostat, the temperature was regulated to within ±1 K, between 298 and 245 K and UV spectra were recorded.

Reagent pressures were selected taking into account two opposing features. On the one hand, the need to avoid condensation within the cell at low temperatures and, on the other hand the need to keep the absorbance between 0.3 and 0.8 to minimize photometric errors when this was possible. The baseline drift with temperature was less than 1×10^{-3} absorbance units.

In order to determine the primary process of the photochemical rupture of trifluoromethoxycarbonyl peroxy nitrate and the products formed, a double walled quartz IR gas cell (optical path 21 cm) mounted in the optical path of a Bruker IFS-66v FTIR spectrometer was employed. The cell was thermostatized circulating commercial ethanol in the surrounding doubled wall. To prevent the condensation of water on cell's windows, the FTIR cavity was sealed and evacuated. The temperature was regulated to within ±1 K between 297 and 253 K using a Lauda cryostat.

Perfluoroacetic anhydride was used as actinometer to quantify the incident photon flux at the infrared cell. The values were used to determine the quantum yields of trifluoromethoxycarbonyl peroxy nitrate. The procedure was repeated prior to each photolysis at different temperatures.

Atmospheric lifetimes with respect to photolysis were calculated using the TUV 4.2 program [14] as a function of altitude and solar zenith angle. A pressure independent quantum yield of unity at all wavelengths was assumed to run the TUV program, though we have measured the quantum yield at 254 nm.

The other program used to analyze the progress of photolysis of the peroxynitrate in the reaction cell as function of time (that included all the different conditions) was the kinetic model KINTECUS, available at www.kintecus.com.

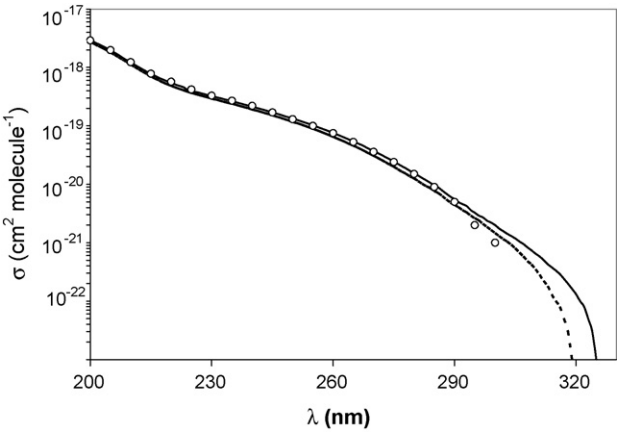

Fig. 1. Absorption cross-sections of $CF_3OC(O)OONO_2$ as a function of wavelength (resolution 1 nm) obtained at two temperatures: solid line (297 K), dotted line (245 K). Circles correspond to values obtained by von Ahsen et al. [6].

3. Results and discussion

3.1. UV temperature dependence

The determination of the UV absorption cross-sections for trifluoromethoxycarbonyl peroxynitrate and their dependence with temperature was carried out as described in Malanca et al. [13]. Fig. 1 shows the UV cross-sections at two different temperatures (297 and 245 K) with 1 nm resolution and their comparison with data obtained by von Ahsen et al. [6] at 298 K. As it can be seen the increase of the UV cross-sections with temperature and the agreement of our data with those reported by von Ahsen et al. [6] is clear though there is a small but steady difference at wavelengths longer than 285 nm. The data reported by von Ahsen et al. (0.5, 0.2 and 0.1 at 290, 295 and 300 nm, respectively), contain only one significant digit and consequently their experimental error should be broader than ours which are reported with two significant digits (see Table 1). Moreover, we have extended the range of measurements up to 320 nm without any abrupt change in the cross-sections; that is, there is a smooth continuation. The increase in cross-sections values with temperature is consistent with an increased population of the vibrational and rotational levels of the ground electronic state of the molecule at higher temperatures [15].

The temperature dependence of UV cross-sections (averaged every 5 nm) is presented in Table 1. As it can be seen there is a genuine dependence of the cross-sections with temperature (see that the change is greater than the error values shown in brackets). The dependence is more pronounced towards the longer wavelength tail. The representation of $\log_{10}\sigma = B \times T + \log_{10}\sigma_0$ as a function of temperature (σ and σ_0 are the cross-sections in cm^2 $molecule^{-1}$ at a particular temperature and $T = 0$ K, respectively) gives straight lines. The intercepts (σ_0) and slopes (B) obtained by linear regression analysis for some selected wavelengths are given in Table 2. Note that B increases with wavelength as a consequence of the larger temperature dependence at longer wavelengths. The coefficients derived from the plot can be used to obtain cross-sections values outside the experimental range by extrapolation.

3.2. Products identification and kinetic mechanism

The photolysis of $CF_3OC(O)OONO_2$ at 254 nm could lead a priori to the O–O or O–N bond rupture:

$$CF_3OC(O)OONO_2 + h\nu(\lambda = 254\,\text{nm}) \rightarrow CF_3OC(O)OO + NO_2 \quad (2a)$$

$$CF_3OC(O)OONO_2 + h\nu(\lambda = 254\,\text{nm}) \rightarrow CF_3OC(O)O + NO_3 \quad (2b)$$

Table 1
Absorption cross-sections values (averaged every 5 nm) at different temperatures. The table includes also the value at 254 nm used to determine the quantum yield in this work.

λ (nm)	297 K	285 K	273 K	261 K	245 K
Absorption cross-sections values as a function of temperature					
200	291(3)	286	281	276	271
205	197(3)	193	189	185	182
210	123(3)	120	118	115	114
215	79(2)	77	75	72	71
220	55(2)	53	52	50	49
225	41(2)	40	39	38	37
230	33(1)	32	31	30	29
235	27(1)	26	25	25	24
240	21(1)	21	20	20	19
245	17(1)	17	16	16	15
250	13(1)	13	13	12	12
254	**10.8(0.9)**	**10.4**	**10.1**	**9.8**	**9.5**
255	10.2(0.9)	9.9	9.6	9.2	8.9
260	7.6(0.7)	7.3	7.0	6.8	6.5
265	5.4(0.4)	5.2	5.0	4.8	4.6
270	3.7(0.2)	3.5	3.4	3.2	3.1
275	2.5(0.1)	2.3	2.2	2.1	2.0
280	1.6(0.1)	1.5	1.4	1.3	1.3
285	1.0(0.1)	0.9	0.9	0.8	0.8
290	0.56(0.09)	0.55	0.51	0.48	0.45
295	0.34(0.05)	0.32	0.30	0.28	0.27
300	0.20(0.04)	0.19	0.18	0.16	0.15
305	0.12(0.03)	0.11	0.10	0.09	0.08
310	0.07(0.03)	0.06	0.05	*0.04*	*0.03*
315	*0.03*	*0.03*	*0.02*	*0.02*	*0.01*
320	*0.01*	*0.009*	*0.005*	*0.002*	0
325	*0.002*	0	0	0	0
330	0	0	0	0	0

The bracketed values correspond to one standard deviation. Units are 10^{-20} cm^2 molecule^{-1}. Values in italics are derived from absorbance readings close to the baseline drift, having therefore high relative errors.

Table 2
Parameters (slopes and intercepts) from the linear dependence of cross-sections with temperature at different wavelengths.

λ (nm)	B ($\times 10^3$ K^{-1})	σ_0 ($\times 10^{20}$ cm^2 molecule^{-1})
290	1.9 (0.2)	0.151 (0.008)
295	2.0 (0.2)	0.085 (0.004)
300	2.5 (0.2)	0.035 (0.002)
305	3.43 (0.06)	0.0115 (0.0002)
310	7.2 (0.3)	5.3 (0.4) $\times 10^{-4}$
315	9 (2)	–
320	20 (5)	–

Bracketed values correspond to one standard deviation.

In order to determine the total quantum yield for the photochemical rupture of $CF_3OC(O)OONO_2$ ($\phi = \phi_{NO_2} + \phi_{NO_3}$) the photolysis of $CF_3OC(O)OONO_2$ (0.5 mbar) was carried out in the presence of NO (4.0 mbar) adding N_2 to obtain a total pressure of 100 mbar.

The addition of NO prevents the recombination of the radicals formed in the primary steps (2a) and (2b) through reactions (3) and (4):

$$CF_3OC(O)OO + NO \rightarrow CF_3OC(O)O + NO_2 \quad (3)$$

$$NO_3 + NO \rightarrow NO_2 + NO_2 \quad (4)$$

Though the rate constant k_3 has not actually been measured, a rough estimation of its magnitude was derived from the measurement of the thermal decomposition at room temperature of $CF_3OC(O)OONO_2$ reported in Manetti et al. [12]. There, the authors reported an assumed value of $k_3 = 6.6 \times 10^{-12}$ cm^3 molecule^{-1} s^{-1} (similar to that of the reaction $CF_3C(O)OO + NO$) with which they experimentally avoided the back reaction (−2a) and were able to fit their results to a kinetic model. In turn, k_4 also adopts a high value

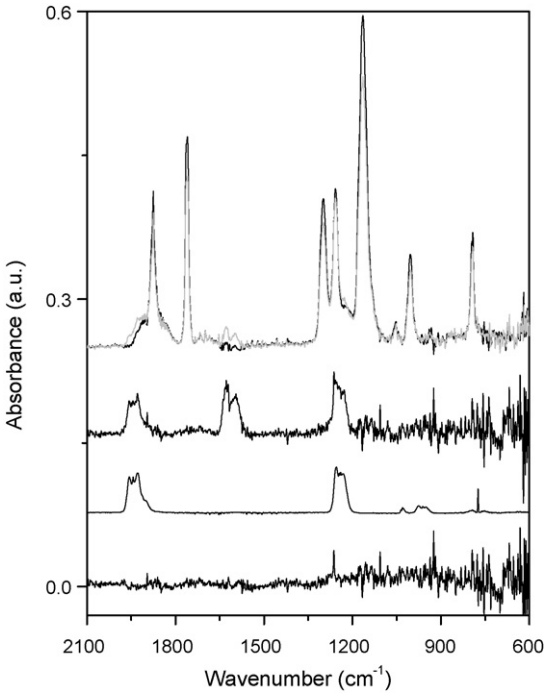

Fig. 2. IR spectra obtained in the photolysis of 0.5 mbar $CF_3OC(O)OONO_2$ in the presence of NO (4.0 mbar) and of N_2 at 1.0 atm total pressure and 297 K. Top to bottom, traces correspond to: First: (black) $t = 0$ and (grey) after 10 min of irradiation. Second: products. Third: reference spectrum of CF_2O. Fourth: Residuals obtained after CF_2O and NO_2 subtraction. As it can be seen there is no evidence of $CF_3OC(O)OOC(O)OCF_3$ formation.

as reported by Sander et al. [16] where the rate constant equals 2.6×10^{-11} cm^3 molecule^{-1} s^{-1}.

Channel (2a) gives the same products as the thermal decomposition. This fact poses a constraint in the quantification of the products formed since it is difficult to know which source they are coming from if IR detection is used. To overcome this problem, two strategies can be adopted. First, prior to a photolytic experiment, the corresponding thermal decomposition has to be carried out and the concentration of products formed subtracted from that of the photolysis experiment. Second, the photolysis could be carried out at low temperatures where the thermal decomposition is very slow, reducing the error associated to the subtraction. Nevertheless, this requires that the quantum yields have to be measured at those temperatures. We used both strategies and measured the quantum yields at 297, 273, 263 and 253 K.

Besides, as we measured the decomposition in the presence of either NO or cyclohexane to distinguish between channels (2a) and (2b), we could profit from low temperatures when using NO, but we were forced to work at higher temperatures (297 K) when c-C_6H_{12} was used because the lower temperatures do not allow us to reach the amount of c-hexane needed to assure that all NO_3 radicals react.

Fig. 2 shows the spectra obtained in the photolysis of $CF_3OC(O)OONO_2$ in the presence of NO at 273 K. As it can be seen, the formation of CF_2O, as a consequence of subsequent reactions of $CF_3OC(O)O$ radicals formed in reaction (3) is clear.

$$CF_3OC(O)O \rightarrow CF_3O + CO_2 \quad (5)$$

$$CF_3O + NO \rightarrow CF_2O + FNO \quad (6)$$

As FTIR spectra (shown in Fig. 2) reveal, we did not observe the formation of FNO as a stable product, and NO_2 is the only nitrogen-containing product observed. These results agree with the products observed also in our group by Manetti et al. [12] in the thermal decomposition of $CF_3OC(O)OONO_2$ in the presence of NO, where

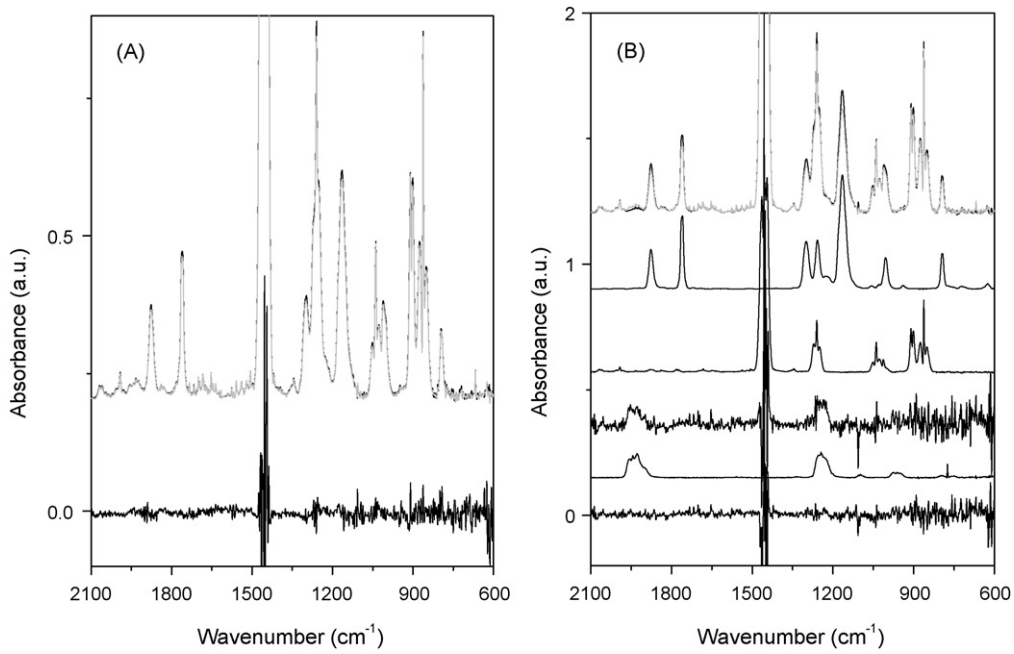

Fig. 3. IR spectra obtained in the thermal decomposition (A) and photolysis (B) of $CF_3OC(O)OONO_2$ in the presence of c-C_6H_{12} at 297 K. From top to bottom: Subset (A): first trace (black, $t = 0$; gray, $t = 80$ min); last trace results from subtraction. As it can be seen there are no signals suggesting the formation of products, and therefore the trace corresponds to residuals. Subset (B): first trace (black, $t = 0$; gray, $t = 80$ min); second and third trace, $CF_3OC(O)OONO_2$ and c-C_6H_{12} reference spectra, respectively; fourth trace, products; fifth trace, CF_2O reference spectrum; sixth trace, residuals after appropriate subtraction of c-C_6H_{12}, $CF_3OC(O)OONO_2$ and CF_2O.

it was discussed and concluded that FNO must be converted into HF by hydrolysis at the walls. Therefore, as the experimental set-up is similar, it seems completely reasonable that also here FNO decomposes.

As it can be also seen, the residual spectrum (obtained after subtraction of CF_2O and NO_2 spectra to the corresponding products) does not show other carbonated product.

The high NO concentration used to carry out the photolysis ($1.0–2.0 \times 10^{17}$ molecule cm^{-3}) and the low conversion of $CF_3OC(O)OONO_2$ guarantee that the NO_2 formed through reactions (2a) and (3) and (4) does not react with the $CF_3OC(O)OO$ radicals to re-form the trifluoromethoxycarbonyl peroxy nitrate. This allows the determination of the global quantum yield; but it is not possible to establish whether the rupture occurs via (2a), (2b) or both. As mentioned before, the elucidation of their relative importance was done by carrying out the photolysis of $CF_3OC(O)OONO_2$ in the presence of excess cyclohexane, which reacts with NO_3 radicals (reaction (7)):

$$NO_3 + \text{c-}C_6H_{12} \rightarrow \text{ Products} \quad (7)$$

The rate constant for reaction (7) at 298 K has been measured by Atkinson et al. [17], $k_7 = (1.3 \pm 0.3) \times 10^{-16}$ cm^3 $molecule^{-1}$ s^{-1}. The available rate data are consistent with a mechanism in which an H-atom is abstracted from a C–H bond as in reaction (8) [18]

$$NO_3 + RH \rightarrow HNO_3 + R \quad (8)$$

Given the relatively low rate constant, the capture of NO_3 radicals by cyclohexane required a pressure of about 90 mbar. Therefore, the photolysis of $CF_3OC(O)OONO_2$ had to be carried out at room temperature where the vapor pressure of c-C_6H_{12} is close to this value. Here again, the contribution of the thermal decomposition of $CF_3OC(O)OONO_2$ during the photolysis was checked. Fig. 3 shows the IR spectra obtained in the thermal decomposition (A) and photolysis (B) of $CF_3OC(O)OONO_2$ in the presence of c-C_6H_{12} at 297 K. As it can be seen there is a measurable, though not substantial, disappearance of trifluoromethoxycarbonyl peroxy nitrate without light, leading to the conclusion that some type of reaction between NO_2 or $CF_3OC(O)OO$ and c-C_6H_{12} occurs but neither of them reacting sufficiently fast so as to compete with reaction (−2a). Kinetic data for the reaction between $CF_3OC(O)OO$ radicals and cyclohexane have not been reported yet. When lamps were turned on, reaction (2b) occurred leading to NO_3 formation, which is trapped by cyclohexane through reaction (7). The analysis of the infrared spectra shows that the only carbon product formed is CF_2O formed via reactions (5) and (6).

Fig. 4 shows the temporal variation in the concentration of $CF_3OC(O)OONO_2$ for the different experiments performed. The photolytic reaction at room temperature in the presence of added gases adopts its higher value for NO as compared to the corresponding process in cyclohexane. When comparing the temperature dependence, the disappearance of trifluoromethoxycarbonyl peroxy nitrate is higher at 297 K. When the temperature is lowered,

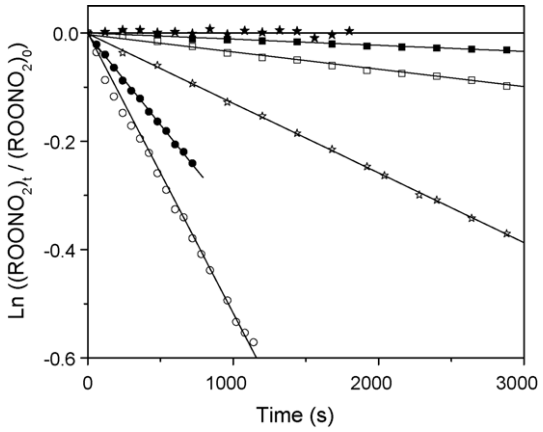

Fig. 4. Temporal variation of the concentration of $CF_3OC(O)OONO_2$ (labeled as $ROONO_2$). Solid and open symbols correspond to thermal and photolytic decomposition. Circles and stars represent the decomposition, respectively in the presence of NO at 297 and 253 K, respectively. Squares represent the decomposition in the presence of c-C_6H_{12} at 297 K.

Table 3
Kinetic model used to fit the experimental data. In each case, p_{total} = 100 Torr was obtained adding N_2. Values listed in columns 3–6 were obtained through a sensitivity analysis. Columns 3 and 4 summarize the thermal and photochemical studies in the presence of NO. Columns 5 and 6 are the equivalent for c-C_6H_{12}.

Reaction	Rate constant[a] $k_{(298K)}$	NO Δ	NO $h\nu$	Chx Δ	Chx $h\nu$	References
$CF_3OC(O)OONO_2 + h\nu \rightarrow CF_3OC(O)OO + NO_2$	1.56×10^{-4}	–	28.8	–	1.6	This work
$CF_3OC(O)OONO_2 + h\nu \rightarrow CF_3OCOO + NO_3$	3.2×10^{-5}	–	6.0	–	84.6	This work
$CF_3OC(O)OONO_2 \rightarrow CF_3OC(O)OO + NO_2$	3.45×10^{-4}	98.8	63.6	25.8	3.5	This work
$CF_3OC(O)OO + NO_2 \rightarrow CF_3OC(O)OONO_2$	6.6×10^{-12}	0.6	0.8	25.0	5.1	A
$2\ CF_3OC(O)OO \rightarrow 2\ CF_3OCOO + O_2$	9.3×10^{-12}	<0.1	<0.1	12.6	2.6	B
$CF_3OCOO + CF_3OCOO \rightarrow CF_3O(O)OOC(O)OCF_3$	1.4×10^{-11}	<0.1	<0.1	6.6	<0.1	C
$CF_3OCOO \rightarrow CF_3O + CO_2$	40	<0.1	<0.1	13.2	<0.1	[12]
$CF_3O + NO_2 \rightarrow CF_3ONO_2$	1.3×10^{-11}	<0.1	<0.1	0.1	<0.1	[6]
$CF_3ONO_2 + wall \rightarrow CF_2O + FNO_2$	> 0.02	<0.1	<0.1	7.0	<0.1	This work
$FNO_2 + wall \rightarrow HF + NO_2$	9.4×10^{-3}	<0.1	<0.1	9.6	<0.1	D
$NO_3 + NO_2 \rightarrow N_2O_5$	7.9×10^{-13}	–	<0.1	–	0.3	[16]
$NO_3 + NO_2 \rightarrow NO_2 + NO + O_2$	6.3×10^{-16}	–	<0.1	–	<0.1	[16]
$NO_2 + h\nu \rightarrow NO$	3.4×10^{-5}	–	<0.1	–	0.1	E
$CF_3OCOO + NO_3 \rightarrow CF_3OC(O)OO + NO_2$	3.3×10^{-12}	–	<0.1	–	<0.1	F
$CF_3OC(O)OO + NO_3 \rightarrow CF_3OCOO + NO_2 + O_2$	2.3×10^{-12}	–	<0.1	–	<0.1	F
$CF_3OC(O)OO + NO \rightarrow CF_3OCOO + NO_2$	2.6×10^{-11}	0.6	0.8	–	<0.1	B
$NO_3 + NO \rightarrow 2NO_2$	2.6×10^{-11}	–	<0.1	–	<0.1	[16]
$CF_3O + NO \rightarrow CF_2O + FNO$	5.3×10^{-11}	<0.1	<0.1	–	<0.1	[19]
$N_2O_5 + h\nu \rightarrow NO_2 + NO_3$	5.5×10^{-4}	–	<0.1	–	<0.1	E
$N_2O_5 \rightarrow NO_2 + NO_3$	0.025	–	<0.1	–	0.3	G
$NO_3 + NO_3 \rightarrow NO_2 + NO_2 + O_2$	2.3×10^{-16}	–	<0.1	–	<0.1	[16]
$NO_3 + c\text{-}C_6H_{12} \rightarrow HNO_3 + c\text{-}C_6H_{11}$	1.35×10^{-16}	–	–	–	0.3	[17]
$CF_3O + c\text{-}C_6H_{12} \rightarrow CF_3OH + c\text{-}C_6H_{11}$	6.8×10^{-12}	–	–	<0.1	<0.1	H
$CF_3OH \rightarrow CF_2O + HF$	0.40	–	–	<0.1	<0.1	I
$c\text{-}C_6H_{11} + c\text{-}C_6H_{11} \rightarrow$ products	3.0×10^{-11}	–	–	<0.1	<0.1	[20]
$c\text{-}C_6H_{11}O \rightarrow$ products	152	–	–	<0.1	<0.1	J
$c\text{-}C_6H_{11} + O_2 \rightarrow c\text{-}C_6H_{11}OO$	1.3×10^{-11}	–	–	<0.1	<0.1	[20]
$c\text{-}C_6H_{11}OO + NO_2 \rightarrow c\text{-}C_6H_{11}OONO_2$	9.5×10^{-12}	–	–	<0.1	0.6	[20]
$c\text{-}C_6H_{11}OONO_2 \rightarrow c\text{-}C_6H_{11}OO + NO_2$	4.8	–	–	<0.1	0.6	[21]
$c\text{-}C_6H_{11}OO + c\text{-}C_6H_{11}OO \rightarrow c\text{-}C_6H_{11}O + c\text{-}C_6H_{11}O + O_2$	2.4×10^{-14}	–	–	<0.1	0.3	[22]
$c\text{-}C_6H_{11}O + O_2 \rightarrow$ cyclohexanone	1.88×10^{-14}	–	–	<0.1	<0.1	[23]
$FNO + wall \rightarrow HF +$ products	>0.05	<0.1	<0.1	–	<0.1	[12]

[a] First-order reactions, in s^{-1}; second-order reactions, in cm^3 $molecule^{-1}$ s^{-1}. [A,B,C]From Manetti et al. [12]. The authors assumed the rate constant as similar to those reported for the $CF_3C(O)OO$ radical measured by [A]Wallington et al. [24], [B]Maricq et al. [25], and for the CF_3OO radical measured by [C]Nielsen et al. [26]. [D]Measured in our laboratory adding FNO_2 to the glass cell used to run the experiments. [E]Calculated using data of photon flux determined by actinometry; UV cross-sections ($\sigma_{NO_2} = 2.0 \times 10^{-20}$ cm^2 $molecule^{-1}$) [16], ($\sigma_{N_2O_5} = 32.6 \times 10^{-20}$ cm^2 $molecule^{-1}$) [27] and quantum yields at 254 nm (ϕ = 1.00) [16]. [F]Assumed to be similar to the reactions between NO_3 and C_2H_5O or C_2H_5OO radicals measured by Ray et al. [28]. [G]Calculated using data of recombination of NO_3 and NO_2 radicals and K_{eq} reported in Sander et al. [16]. [H]Assumed to be similar to the reactions between CF_3O radical and $(CH_3)_3CH$ measured by Barone et al. [29]. [I]Adjusted using the minimum value to account for the non-observation of CF_3OH. [J]Calculated using the ratio for the rupture of c-$C_6H_{11}O$ and the reaction with O_2 from Platz et al. [20] and the rate constant for the reaction of this radical with O_2 from Zhang et al. [23].

the thermal decomposition becomes non-significant and the disappearance of trifluoromethoxycarbonyl peroxy nitrate is obtained only through the photochemical process. This contribution can also be obtained at every temperature by subtracting the slopes of the open (photochemical + thermal) minus the solid (thermal) symbols. Intermediate temperatures, not shown in the figure., do provide the information outlined (as we will discuss later, the dependence of cross-sections with temperature was taken into account). The set of squares in the figure corresponds to the comparison between thermal and photochemical decomposition in the presence of an excess cyclohexane. This particular process with this particular added gas is the one that provides the quantum yield for channel (2b) since the NO_3 radicals effectively react with c-C_6H_{12} abstracting an H atom.

As we have essentially two different systems that share some reactions, the behavior of any of them should be reproduced, within the frame of a kinetic model, using a unique set of rate constants. We have used the Kintecus program (available at www.kintecus.com) to model the temporal variation in the concentration of trifluoromethoxycarbonyl peroxy nitrate at room temperature for all the different possibilities adopted for our systems; that is, with and without light.

Table 3 lists the set of reactions used (column 1) with the values adopted for every single rate constant (column 2) whose source is referred in the last column. The values were, as usual, taken from the literature (when available); assumed, for some specific reactions not measured so far; determined in the present work; or adjusted by the model to get the best possible fit to the experimental concentration of reagents and products. Additionally, sensitivity analyses were carried out for each condition to highlight the relative importance of each reaction rate in the system and these values are the numbers in columns 3–6. A simple analysis shows that the thermal decomposition of the trifluoromethoxycarbonyl peroxy nitrate in the presence of NO has only one important reaction, which is the decomposition itself. In the case of the photochemical decomposition (also in the presence of NO), besides the thermal contribution, only the two photochemical paths are relevant. In the presence of cyclohexane, both decomposition and re-formation reactions of trifluoromethoxycarbonyl peroxy nitrate are important in the absence of light. When the lights are on, it is immediately clear that the production of NO_3 radicals acquires importance while the formation of NO_2 (thermal and photochemical) decrease their participation because of the increasing importance of the recombination to give back the original peroxynitrate.

3.3. Quantum yield determination

The determination of quantum yields was carried out using trifluoroacetic anhydride as actinometer as described in Chiappero et al. [30]. Due to the fact that photolysis were carried out at low temperatures, the dependence of the UV absorption cross-section of the actinometer at 254 nm ($\sigma = 2.28 \pm 0.03) \times 10^{-19}$ cm^2 $molecule^{-1}$, $\phi = 0.29 \pm 0.02$) [31] between 297 and 245 K, was measured. There was no dependence with temperature, within our experimental errors.

Table 4 lists the values of total quantum yield (obtained in the presence of NO) and the corresponding ϕ for NO_3 formation

Table 4
Quantum yields for the photolysis of $CF_3OC(O)OONO_2$ determined at room and low temperatures. NO and c-C_6H_{12} were added to trap the radicals formed (see text for details). The experiments were carried out adding N_2 to obtain a total pressure of 100 Torr.

Gas added p (mbar)	T (K)	ϕ_T			ϕ_{NO_3}		
		$\phi_{CF_3OC(O)OONO_2}$	ϕ_{CF_2O}	ϕ_{PROM}	$\phi_{CF_3OC(O)OONO_2}$	ϕ_{CF_2O}	$\phi_{average}$
NO (4.0 mbar)	298	1.04 ± 0.09	0.94 ± 0.07	0.99 ± 0.09	–	–	–
NO (4.0 mbar)	273	1.01 ± 0.09	1.02 ± 0.08	1.01 ± 0.09	–	–	–
NO (4.0 mbar)	263	1.00 ± 0.08	0.98 ± 0.08	0.99 ± 0.08	–	–	–
NO (4.0 mbar)	253	1.04 ± 0.09	1.02 ± 0.09	1.03 ± 0.09	–	–	–
c-C_6H_{12} (90 mbar)	298	–	–	–	0.17 ± 0.02	0.16 ± 0.02	0.17 ± 0.02
c-C_6H_{12} (90 mbar)	298	–	–	–	0.21 ± 0.04	0.19 ± 0.03	0.20 ± 0.03

(obtained in the presence of c-C_6H_{12}). The overall values listed are 1.01 ± 0.09 and 0.18 ± 0.03, respectively. The quantification was carried out using two criteria. On the one hand, we measured the disappearance of trifluoromethoxycarbonyl peroxy nitrate exclusively and listed the results derived for ϕ in columns 3 and 6. On the other hand, we followed and quantified the appearance of CF_2O (the only carbonated product) and the values for ϕ calculated form this species were listed in columns 4 and 7. As it can be seen the results obtained in both ways agree within the experimental errors.

Several results for ϕ_{NO_3} of related peroxynitrates have been reported. Those of Mazely et al. [7,8] who reported a value of 0.3 ± 0.1 for PAN were the first measurements. Later, Harwood et al. [9] reported values of 0.19 ± 0.04 and 0.22 ± 0.04 for PAN and PPN, respectively. Comparing our results with those obtained for different peroxynitrates, it can be suggested that, ϕ_{NO_3} for $RC(O)OONO_2$ (R = CH_3–PAN–,C_2H_5–PPN– and CF_3O-trifluoromethoxycarbonyl peroxy nitrate-) is similar within experimental errors.

3.4. Atmospheric implications

Fig. 5 shows the lifetime of $CF_3OC(O)OONO_2$ and its dependence with altitude and latitude for 0°, 30° and 60°. The photochemical lifetimes have been calculated as the result of the average for 4 selected days; 2 solstices and 2 equinoxes. As expected, the photochemical lifetime is a function of both altitude and latitude, being the maximum at each latitude higher than 100 days and reaching the higher values toward higher latitudes. The maximum in altitude is reached at around 7–8 km for all the latitudes as a consequence of the counteracting effects of the decrease in absorption cross-sections with temperature and the increase in solar flux with altitude. Above the tropopause, both the cross-sections and the solar flux increase and consequently the photochemical lifetime steadily decreases.

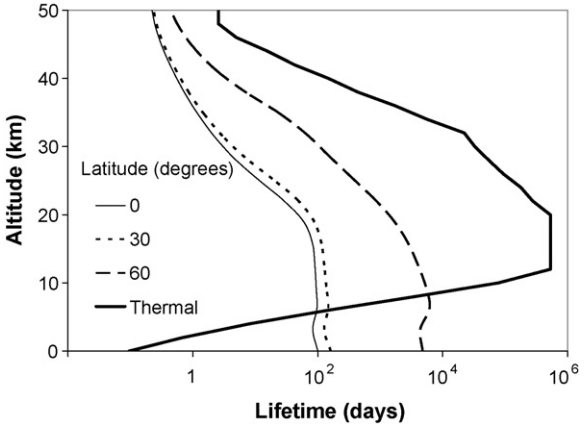

Fig. 5. Thermal (taken from Manetti et al. [12]) and photochemical lifetime profiles for $CF_3OC(O)OONO_2$ at different latitudes.

On the other hand, the thermal lifetime for $CF_3OC(O)OONO_2$ increases substantially with altitude up to around 12 km due to the decrease in temperature and is maximum at the tropopause where it is of the order of several years. Above the tropopause, the thermal lifetime decreases as a consequence of the increase in temperature within the stratosphere.

The comparison of the thermal and the photochemical lifetime leads to the following conclusions which are similar to those obtained for other peroxynitrates. Altogether, from the surface up to 5 km, loss via thermal decomposition dominates over photolytic losses; from around 5 km up, the photochemical rupture is the dominant loss process. That is, the lifetime from the surface up increases while the dissociation is controlled by the thermal process; when this curve crosses the photochemical one, the control shifts and the lifetime begins to decrease. Therefore the lifetime of $CF_3OC(O)OONO_2$ in the free troposphere, favors its transport and distribution to non-production zones of the atmosphere, since the crossing point where the control of the residence time changes – around 7 km altitude – occurs for lifetimes of ca. 3 months, sufficient to allow a broad dispersion and distribution following the movement of air masses.

Acknowledgement

Financial support from CONICET, SECYT-UNC and FONCYT, is gratefully acknowledged.

References

[1] M.K.W. Ko, N.D. Sze, J.M. Rodriguez, D.K. Weistenstein, C.W. Heisey, R.P. Wayne, P. Biggs, C.E. Canosa-Mas, H.W. Sidebottom, J. Treacy, CF_3 chemistry: potential implications for stratospheric ozone, Geophys. Res. Lett. 21 (1994) 101–104.
[2] R.K. Talukdar, J.B. Burkholder, A.-M. Schmoltner, J.M. Roberts, R.R. Wilson, A.R. Ravishankara, Investigation of the loss processes for peroxyacetyl nitrate in the atmosphere: UV photolysis and reaction with OH, J. Geophys. Res. [Atmosph.] 100 (1995) 14163–14173.
[3] F. Kirchner, L.P. Thuener, I. Barnes, K.H. Becker, B. Donner, F. Zabel, Thermal lifetimes of peroxynitrates occurring in the atmospheric degradation of oxygenated fuel additives, Environ. Sci. Technol. 31 (1997) 1801–1804.
[4] R. Atkinson, S.M. Aschmann, A.M. Winer, W.P.L. Carter, Rate constants for the gas phase reactions of hydroxyl radicals and ozone with pyrrole at 295 ± 1 K and atmospheric pressure, Atmosph. Environ. 18 (1984) 2105–2107.
[5] F. Caralp, V. Foucher, R. Lesclaux, T.J. Wallington, M.D. Hurley, Atmospheric chemistry of benzaldehyde: UV absorption spectrum and reaction kinetics and mechanisms of the $C_6H_5C(O)O_2$ radical, Phys. Chem. Chem. Phys. 1 (1999) 3509–3517.
[6] S. von Ahsen, P. Garcia, H. Willner, G.A. Argüello, Trifluoromethoxycarbonyl peroxynitrate, $CF_3OC(O)OONO_2$, Inorg. Chem. 44 (2005) 5713–5718.
[7] T.L. Mazely, R.R. Friedl, S.P. Sander, Production of NO_2 from photolysis of peroxyacetyl nitrate, J. Phys. Chem. A 99 (1995) 8162–8169.
[8] T.L. Mazely, R.R. Friedl, S.P. Sander, Quantum yield of NO_3 from peroxyacetyl nitrate photolysis, J. Phys. Chem. A 101 (1997) 7090–7097.
[9] M.H. Harwood, J.M. Roberts, G.J. Frost, A.R. Ravishankara, J.B. Burkholder, Photochemical studies of $CH_3C(O)OONO_2$ (PAN) and $CH_3CH_2C(O)OONO_2$ (PPN): NO_3 quantum yields, J. Phys. Chem. A 107 (2003) 1148–1154.
[10] B.A. Flowers, J.F. Stanton, W.R. Simpson, Wavelength dependence of nitrate radical quantum yield from peroxyacetyl nitrate photolysis: experimental and theoretical studies, J. Phys. Chem. A 111 (2007) 11602–11607.
[11] L.K. Christensen, T.J. Wallington, A. Guschin, M.D. Hurley, Atmospheric degradation mechanism of CF_3OCH_3, J. Phys. Chem. A 103 (1999) 4202–4208.

[12] M. Manetti, F.E. Malanca, G.A. Argüello, Thermal decomposition of trifluoromethoxycarbonyl peroxy nitrate, $CF_3OC(O)O_2NO_2$, Int. J. Chem. Kinet. 40 (2008) 831–838.
[13] F.E. Malanca, M.S. Chiappero, G.A. Argüello, T.J. Wallington, Trifluoro methyl peroxynitrate (CF_3OONO_2): temperature dependence of the UV absorption spectrum and atmospheric implications, Atmosph. Environ. 39 (2005) 5051–5057.
[14] S. Madronich, S. Flocke, The Role of Solar Radiation in Atmospheric Chemistry, Springer, Heidelberg, 1998.
[15] H. Okabe, Photochemistry of Small Molecules, New York, 1978.
[16] S.P. Sander, R.R. Friedl, A.R. Ravishankara, D.M. Golden, C.E. Kolb, M.J. Kurylo, R.E. Huie, V.L. Orkin, M.J. Molina, G.K. Moortgat, B.J. Finlayson-Pitts, Chemical Kinetics and Photochemical Data for Use in Atmospheric Studies. Evaluation Number, vol. 14, Jet Propulsion Laboratory, Pasadena, CA, 2005.
[17] R. Atkinson, S.M. Aschmann, J.N. Pitts Jr., Rate constants for the gas phase reactions of the NO_3 radical with a series of organic compounds at 296 ± 2 K, J. Phys. Chem. 92 (1988) 3454–3457.
[18] R.P. Wayne, I. Barnes, P. Biggs, J.P. Burrows, C.E. Canosa-Mas, J. Hjorth, G. Le Bras, G.K. Moortgat, D. Perner, G. Poulet, G. Restelli, H. Sidebottom, The nitrate radical: physics, chemistry, and the atmosphere, Atmosph. Environ. A: Gen. Topics 25A (1991) 1–203.
[19] R. Atkinson, D.L. Baulch, R.A. Cox, J.N. Crowley, R.F. Hampson Jr., J.A. Kerr, M.J. Rossi, J. Troe, Summary of evaluated kinetic and photochemical data for atmospheric chemistry, IUPAC Subcommittee on Gas Kinetic Data Evaluation for Atmospheric Chemistry Web Version, December 2001, pp. 1–56.
[20] J. Platz, J. Sehested, O.J. Nielsen, T.J. Wallington, Atmospheric chemistry of cyclohexane: UV spectra of c-C_6H_{11} and (c-C_6H_{11})O_2· radicals, kinetics of the reactions of (c-C_6H_{11})O_2· radicals with NO and NO_2, and the fate of the alkoxy radical (c-C_6H_{11})O·, J. Phys. Chem. A 103 (1999) 2688–2695.
[21] F. Kirchner, A. Mayer-Figge, F. Zabel, K.H. Becker, Thermal stability of peroxynitrates, Int. J. Chem. Kinet. 31 (1999) 127–144.
[22] D.M. Rowley, P.D. Lightfoot, R. Lesclaux, T.J. Wallington, UV absorption spectrum and self-reaction of cyclohexylperoxy radicals, J. Chem. Soc., Faraday Trans. 87 (1991) 3221–3226.
[23] L. Zhang, K.A. Kitney, M.A. Ferenac, W. Deng, T.S. Dibble, LIF spectra of cyclohexoxy radical and direct kinetic studies of its reaction with O_2, J. Phys. Chem. A 108 (2004) 447–454.
[24] T.J. Wallington, J. Sehested, O.J. Nielsen, Atmospheric chemistry of $CF_3C(O)O_2$ radicals. Kinetics of their reaction with NO_2 and kinetics of the thermal decomposition of the product $CF_3C(O)O_2NO_2$, Chem. Phys. Lett. 226 (1994) 563–569.
[25] M.M. Maricq, J.J. Szente, G.A. Khitrov, J.S. Francisco, The $CF_3C(O)O_2$ radical. Its UV spectrum, self-reaction kinetics, and reaction with NO, J. Phys. Chem. 100 (1996) 4514–4520.
[26] O.J. Nielsen, T. Ellermann, J. Sehested, E. Bartkiewicz, T.J. Wallington, M.D. Hurley, UV absorption spectra, kinetics, and mechanisms of the self reaction of CF_3O_2 radicals in the gas phase at 295 K, Int. J. Chem. Kinet. 24 (1992) 1009–1021.
[27] M.H. Harwood, J.B. Burkholder, A.R. Ravishankara, Photodissociation of $BrONO_2$ and N_2O_5: quantum yields for NO_3 production at 248 308 and 352.5 nm, J. Phys. Chem. A 102 (1998) 1309–1317.
[28] A. Ray, V. Daele, I. Vassalli, G. Poulet, G. Le Bras, Kinetic study of the reactions of C_2H_5O and $C_2H_5O_2$ with NO_3 at 298 K, J. Phys. Chem. 100 (1996) 5737–5744.
[29] S.B. Barone, A.A. Turnipseed, A.R. Ravishankara, Kinetics of the reactions of the CF_3O radical with alkanes, J. Phys. Chem. 98 (1994) 4602–4608.
[30] M.S. Chiappero, F.E. Malanca, G.A. Argüello, S.T. Wooldridge, M.D. Hurley, J.C. Ball, T.J. Wallington, R.L. Waterland, R.C. Buck, Atmospheric chemistry of perfluoroaldehydes ($C_xF2_{x+1}CHO$) and fluorotelomer aldehydes ($C_xF_{2x+1}CH_2CHO$): quantification of the important role of photolysis, J. Phys. Chem. A 110 (2006) 11944–11953.
[31] G.A. Chamberlain, E. Whittle, Photochemistry of anhydrides. Part 1.—Photolysis of perfluoroacetic anhydrides vapour: a new source of CF_3 radicals, Trans. Faraday Soc. (1971) 88–95.